# Functions of c-Jun in Liver and Heart Development

**Robert Eferl,* Maria Sibilia,‡ Frank Hilberg,§ Andrea Fuchsbichler,* Iris Kufferath,* Barbara Guertl,* Rainer Zenz,* Erwin F. Wagner,‡ and Kurt Zatloukal***

*Department of Pathology, University of Graz, A-8036 Graz, Austria; ‡Research Institute of Molecular Pathology, A-1030 Vienna, Austria; and §Boehringer Ingelheim, A-1121 Vienna, Austria

*Abstract.* Mice lacking the AP-1 transcription factor c-Jun die around embryonic day E13.0 but little is known about the cell types affected as well as the cause of embryonic lethality. Here we show that a fraction of mutant E13.0 fetal livers exhibits extensive apoptosis of both hematopoietic cells and hepatoblasts, whereas the expression of 15 mRNAs, including those of albumin, keratin 18, hepatocyte nuclear factor 1, β-globin, and erythropoietin, some of which are putative AP-1 target genes, is not affected. Apoptosis of hematopoietic cells in mutant livers is most likely not due to a cell-autonomous defect, since *c-jun*$^{-/-}$ fetal liver cells are able to reconstitute all hematopoietic compartments of lethally irradiated recipient mice. A developmental analysis of chimeras showed contribution of *c-jun*$^{-/-}$ ES cell derivatives to fetal, but not to adult livers, suggesting a role of c-Jun in hepatocyte turnover. This is in agreement with the reduced mitotic and increased apoptotic rates found in primary liver cell cultures derived from *c-jun*$^{-/-}$ fetuses. Furthermore, a novel function for c-Jun was found in heart development. The heart outflow tract of *c-jun*$^{-/-}$ fetuses show malformations that resemble the human disease of a truncus arteriosus persistens. Therefore, the lethality of *c-jun* mutant fetuses is most likely due to pleiotropic defects reflecting the diversity of functions of c-Jun in development, such as a role in neural crest cell function, in the maintenance of hepatic hematopoiesis and in the regulation of apoptosis.

Key words: apoptosis • neural crest • hematopoiesis • knockout • truncus arteriosus persistens



THE proto-oncogene *c-jun* encodes a component of the transcription factor AP-1 (activating protein 1)[1], which has been implicated in the regulation of diverse cellular functions, such as proliferation, differentiation, transformation, and apoptosis. AP-1 is a dimer consisting of different subunits, e.g., proteins of the Jun (c-Jun, JunB, and JunD) and Fos (c-Fos, FosB, Fra1, and Fra2) family as well as CREB/ATF, and Maf proteins. The different AP-1 components are expressed in a development- and tissue-specific manner, implying that AP-1 composed of different subunits may exert different functions in different cell types. Although AP-1 was found to regulate a few genes, such as human metallothionein IIA (Lee et al., 1987), collagenase (Angel et al., 1987), stromelysin (Kerr et al., 1988), and keratin 18 (Oshima et al., 1990), the biological function of the different AP-1 complexes during development is still elusive. The characterization of the role of AP-1 is further impeded by the fact that there are, in addition to the variability in subunit composition, numerous possible interactions between AP-1 and other transcription factors, such as glucocorticoid hormone receptors (Jonat et al., 1990), estrogen receptors (Gaub et al., 1990), retinoic acid and vitamin D3 receptors (Schüle et al., 1990), and MyoD (Bengal et al., 1992) yielding a network of transcriptional regulation.

First clues on tissue-specific functions of AP-1 components came from gene knockout experiments. In *c-fos* knockout mice the development of bone is impaired because of a block in osteoclast differentiation (Grigoriadis et al., 1994). Moreover, lymphoid cells, germ cells, and neuronal tissues are affected in the absence of c-Fos (Johnson et al., 1992; Wang et al., 1992). In contrast to the inactivation of *c-fos*, targeted disruption of *c-jun* and *junB* is lethal (Hilberg et al., 1993; Johnson et al., 1993; Schorpp-Kistner et al., 1999). Lethality of *c-jun*$^{-/-}$ fetuses has been suggested to be due to defective liver development. The livers of some E12.5 animals appeared hypoplastic with rounded, dissociated hepatoblasts showing features of apoptosis and necrosis. Moreover, increased

Address correspondence to Kurt Zatloukal, Department of Pathology, Auenbruggerplatz 25, A-8036 Graz, Austria. Tel.: 43 0316 3804404. Fax: 43 0316 384329. E-mail: kurt.zatloukal@kfunigraz.ac.at

1. *Abbreviations used in this paper:* AP-1, activating protein 1; Cx 43, connexin 43; ES cells, embryonic stem cells; GPI, glucose phosphate isomerase; HGF, hepatocyte growth factor; HNF-1, hepatocyte nuclear factor 1; RT-PCR, reverse transcriptase PCR; TUNEL, TdT-mediated dUTP nick-end labeling.

numbers of erythropoietic cells were noted in these livers (Hilberg et al., 1993). A defect in hepatogenesis in c-Jun knockout mice was further indicated by the observation that *c-jun*$^{-/-}$ embryonic stem (ES) cells failed to contribute to the liver but not to other tissues of adult chimeric mice (Hilberg et al., 1993). These observations, together with the fact that no morphological alterations were found in organs other than the liver, led to the conclusion that the absence of c-Jun might preferentially affect the development of the liver (Hilberg et al., 1993).

In the mouse, liver development starts at around E9.5 when epithelial cells of the foregut endoderm proliferate and invade the mesenchyme of the septum transversum thus forming the embryonic liver. At around E11 hematopoietic stem and progenitor cells derived from the yolk sac and aorta-gonad-mesonephros region colonize the liver, and the liver becomes the major hematopoietic organ during further fetal development (Dzierzak and Medvinsky, 1995). To allow establishment and maintenance of hematopoiesis, liver cells have to provide the proper microenvironment for hematopoietic cells comparable to stromal cells in the bone marrow during postnatal life. The next major step in mouse liver development occurs at approximately E14.5 when hepatoblasts start to differentiate into the hepatocytic and bile duct epithelial lineage, which is indicated by the formation of the ductal plate, which later differentiates into the intrahepatic bile ducts (Desmet, 1998). It is as yet unclear at which developmental stage c-Jun becomes essential for the liver, and whether the defect is restricted to the hepatocytic lineage or other cell types of the fetal liver, such as bile duct epithelia, endothelial cells, stellate cells (vitamin A–storing cells), Kupffer cells, and hematopoietic cells.

Besides the poorly characterized function in liver development, c-Jun plays a more general role in the regulation of cell proliferation and apoptosis. It has been shown in fibroblasts isolated from E11.5 *c-jun*$^{-/-}$ and *c-jun*$^{+/-}$ embryos that the absence or diminished expression of c-Jun resulted in greatly reduced growth rates, and that this proliferation defect could not be compensated by addition of purified mitogens (Johnson et al., 1993; Schreiber et al., 1999). Evidence for a role of c-Jun and c-Jun phosphorylation in apoptosis was obtained in neuronal cells where transient overexpression of c-Jun induced apoptosis, and expression of a dominant negative *c-jun* mutant inhibited apoptosis in vitro (Estus et al., 1994; Ham et al., 1995; Behrens et al., 1999). In vivo, however, c-Jun was regarded not to be essential for apoptosis since in the developing mouse (E11.5 *c-jun*$^{-/-}$ fetuses) the physiologically occurring apoptosis appeared unaffected (Roffler-Tarlov et al., 1996).

The different phenotypes observed in the various AP-1 knockout mice point to cell type– and developmental-specific roles of AP-1 complexes. The biological basis for the specific roles is not yet understood. To gain more insight into how the absence of a widely expressed transcription factor like c-Jun affects the liver, and to see whether other tissues are affected, we investigated in detail the morphological and functional alterations in *c-jun* knockout mice as well as the distribution of *c-jun*$^{-/-}$ cells in chimeric mice at various stages during fetal development and postnatal life. A deregulation of apoptosis was found in a variety of cell types lacking *c-jun*, such as hepatoblasts, erythroid cells, and fibroblasts. In contrast to previous reports that suggested that c-Jun is essential for cells to undergo apoptosis, we observed markedly increased apoptotic rates in the absence of c-Jun. It is possible that an increased susceptibility of cells to apoptosis was responsible for the morphologic alterations seen in the livers of *c-jun*$^{-/-}$ mice. Increased apoptotic rates in combination with reduced proliferation rates would result in a disturbance of hepatocyte turnover which could explain the absence of *c-jun*$^{-/-}$ hepatocytes in livers of adult chimeric mice. Furthermore, a novel function of c-Jun in heart development was identified, since all *c-jun*$^{-/-}$ fetuses had a malformation of the outflow tract of the heart which could be a contributing factor to the fetal lethality.

## Materials and Methods

### Mice

Heterozygous *c-jun*$^{+/-}$ male and female mice of C57BL/129 background (Hilberg et al., 1993) were mated and the appearance of the vaginal plug was taken as E0.5. Pregnant mothers were killed at 11.5–14.5 d of gestation by cervical dislocation and the fetuses were isolated. Genotypes of fetuses were determined by PCR using the primers c-jun 1430 and c-jun 2287 (Table I).

### Morphologic and Immunohistochemical Analysis of Fetuses

Mouse fetuses were fixed in 10% phosphate-buffered formaldehyde, paraffin-embedded, and then 4-μm sections were stained with hematoxylin-eosin (HE).

Apoptotic cells were analyzed in paraffin sections by in situ DNA end labeling (TUNEL; Sibilia et al., 1998), and labeled DNA was detected with the ABC procedure (DAKO).

For double-label immunofluorescence analysis fetuses were snap-frozen in isopentane at the temperature of liquid nitrogen, and sections (4 μm thick, fixed in acetone at −20°C for 10 min) were sequentially incubated with the following antibodies: monoclonal mouse antibodies against desmoplakin I and II (Boehringer Mannheim), E-cadherin (ZYMED), connexin 43 (Cx 43; Transduction Laboratories), and monoclonal rat antibodies TER119, CD71, CD11b, and CD34 (PharMingen) against hematopoietic cells or polyclonal rabbit antibodies against desmin (Chemicon) or keratins 8 and 18 (Zatloukal et al., 1990). Primary antibodies were detected with fluorescein isothiocyanate-conjugated or tetramethylrhodamine isothiocyanate-conjugated antibodies directed against mouse and rat or rabbit immunoglobulins, respectively. For negative control, primary antibodies were omitted or replaced by unrelated isotype-matched immunoglobulins. Specimens were analyzed with a MRC600 (Bio Rad Laboratories) laser-scanning confocal device attached to a Zeiss Axiophot microscope. Alternatively, sections of paraffin-embedded liver samples were stained with the antibodies to keratins 8 and 18 or the antibody TER119 after pretreatment with pronase E, and bound antibodies were detected by the APAAP procedure (DAKO).

### Reconstitution of Hematopoiesis in Lethally Irradiated Mice and Flow Cytometric Analysis of Blood Cells

Liver cells isolated from C57BL/129 E12.5 *c-jun*$^{+/-}$ and *c-jun*$^{-/-}$ fetuses were resuspended in PBS, and $10^6$ cells were injected intravenously into adult C57BL/129 wild-type recipient mice that were lethally irradiated (9.5 Gy). All control mice injected with PBS died after 2 wk. After 8 mo, reconstitution of the various hematopoietic lineages was analyzed by FACScan® with the following cell surface markers: B220, CD43, GR1, MAC1, CD4, CD8, TER119, and HSA as described (Sibilia and Wagner, 1995).

### Quantitative RT-PCR

For generation of exogenous artificial RNA standards that served as competitors in quantitative RT-PCR, sequences corresponding to the mRNA or heterologous (unrelated) sequences were cloned into the expression

*Table I. Artificial RNA Standards and Primers for Quantitative RT-PCR*

| mRNA | Standard sequence | Upper primer | Lower primer | Buffer | Reference |
|---|---|---|---|---|---|
| Albumin | 391-584; NcoI (215) | 391-407 | 568-584 | K | Minghetti et al., 1985 |
| Transferrin | 750 bp of 3′ end in vector pmTF-2; NcoI | 5′-TCA ACC TCA CGA CTC CT-3′ | 5′-GCA GCG AAG ACT ACA CC-3′ | A | Ruppert et al., 1990 |
| Keratin 8 | 1299-3′-end; d1317 1348 | 1299-1316 | 1439-1456 | F | Morita et al., 1988 |
| Keratin 18 | 904-3′-end; d921-952 | 904-920 | 1023-1040 | F | Singer et al., 1986 |
| HNF-1 | 1122-1997; AocI (1715) | 1494-1511 | 1765-1782 | J | Kuo et al., 1990 |
| β-Globin | pGEM3Zf (1357-1550) | 38390-38407 | 39436-39453 | N | Shehee et al., 1989 |
| ϵ-Globin | pGEM3Zf (1357-1550) | 9625-9642 | 10482-10499 | N | Shehee et al., 1989 |
| Erythropoietin | 1239-3201; AccI (2365) | 1303-1320 | 3149-3166 | N | Shoemaker et al., 1986 |
| c-jun | 1430-1492/811 bp neo/2205-2304 | 1430-1447 | 2287-2304 | A | Ryder and Nathans, 1988 |
| junB | 1081-1483; d1249-1332 | 1081-1098 | 1466-1483 | J | Ryder et al., 1988 |
| junD | pGEM3Zf (1132-1275) | 519-535 | 732-748 | N | Ryder et al., 1989 |
| c-fos | 2969-3574; AccI (3220) | 2969-2992 | 3551-3574 | J | van Beveren et al., 1983 |
| fosB | 6379-6830; d6418-6592 | 6397-6414 | 6813-6830 | J | Lazo et al., 1992 |
| c-myc | 969-1407; d1003-1186 | 969-986 | 1390-1407 | J | Stanton et al., 1984 |
| Cyclin D2 | 55-520; d228-293 | 55-76 | 502-520 | F | Matsushime et al., 1991 |
| Hepatocyte growth factor | 1186-1748; d1384-1595 | 1186-1203 | 1731-1748 | B | Liu et al., 1993 |
| Glyceraldehyde-3-phosphate dehydrogenase | 326-1152; CelII (510) | 428-445 | 787-804 | L | Sabath et al., 1990 |

Bp numbering corresponds to the published cDNA or genomic DNA sequences. Restriction enzymes used for generation of standards with a mutated restriction site, the positions of the deletions in deletion standards (d) and the positions of the heterologous sequences on plasmid pGEM3z, amplified for heterologous standards, are indicated. In the case of the heterologous standard for *c-jun*, a part of the *c-jun* sequence between bp 1492 and 2205 is replaced by the neomycin resistance gene sequence of transposon TN5 (Hilberg et al., 1993). The indicated buffers correspond to the various PCR buffers of the PCR optimizer kit (Invitrogen).

vector pCRII (Invitrogen; Table I). For restriction standards, a cleavage site of a restriction enzyme between the primer binding sites was mutated by filling it with Klenow fragment (Promega Corp.). Standard plasmids with a deletion between the primer binding sites were constructed either by Bal 31 exonuclease digest or by loop out mutagenesis. For heterologous standards, a heterologous sequence, flanked by the specific primer binding sequences, was generated by amplification with hybrid primers and cloned into pCRII. Exogenous artificial RNA transcripts were generated from linearized standard plasmids by in vitro transcription with the corresponding RNA polymerases (T3, T7, and SP6 were obtained from Boehringer Mannheim). First strand cDNA synthesis for quantitative RT-PCR was performed in a 20-μl reaction mixture containing 0.1 μg of total RNA (isolated as described by Krieg et al., 1983), 0.5 units Inhibit-ACE (5′→3′ Inc.), 1× AMV reverse transcription buffer (100 mM Tris-HCl, pH 8.3 at 42°C, 40 mM KCl, 10 mM $MgCl_2$, and 0.5 mM spermidine), 5 mM dNTPs (1.25 mM each), 4 mM sodium pyrophosphate, 5 units AMV reverse transcriptase (Boehringer Mannheim), 0.5 μM lower primer, and a certain number of exogenous artificial RNA molecules. For PCR optimal buffers for each primer pair were selected using the PCR optimizer kit (Invitrogen; Table I). PCR was performed with one-tenth of the cDNA products amplified in a 50-μl reaction containing 1× PCR buffer, 5 μl DMSO, 1 μM of each primer (except 0.5 μM for quantitation of hepatocyte growth factor mRNA), 0.25 μM of each dNTP, and 2.5 units AmpliTaq DNA Polymerase (Perkin Elmer Cetus). The reaction was heated to 94°C, then Taq Polymerase was added, and subsequently cycled for 45 cycles at 94°C, 1 min, 55°C (except 50°C for albumin and transferrin, 52°C for erythropoietin), 1 min, and 72°C, 1 min. At the end of the last cycle a final extension step of 4 min at 72°C was added. PCR products were separated on ethidium bromide-stained agarose gels and band intensities were estimated by video densitometry (Docu Gel V densitometer and RflpScan or ONE-Dscan software; Scanalytics). mRNA copy numbers were calculated from the differences in the band intensities which were corrected by application of standard curves as described (Eferl et al., 1997).

## *Analysis of Chimeric Mice*

*c-jun*$^{-/-}$ ES cells (clone D3-2, Hilberg et al., 1993) were injected into C57BL/6 blastocysts. Tissues of chimeric mice were analyzed for glucose phosphate isomerase (GPI) isoenzyme distribution as described (Hilberg et al., 1993). The contribution of *c-jun*$^{-/-}$ ES cells to fetal liver tissue was analyzed in short-term cultures of fetal liver cells. Fetal livers were dissected from staged fetuses and after a brief rinse in PBS subjected to 5-min subsequent incubations in solution A (EBSS without $Ca^{2+}$ and $Mg^{2+}$ containing 0.5 mM EGTA), solution B (EBSS containing $Ca^{2+}$, $Mg^{2+}$, and 10 mM Hepes, pH 7.4), and solution C (EBSS containing $Ca^{2+}$, $Mg^{2+}$, 10 mM Hepes, pH 7.4, and 0.3 mg/ml collagenase). Fetal livers were washed once in PBS and liver cells were dispersed by pipetting several times with a 1-ml glass pipette. After centrifugation, cells were cultured in plastic dishes (Falcon Primaria, Becton Dickinson) in DMEM containing 10% fetal calf serum for 2–3 d and nonadherent hematopoietic cells were removed by repeated washings twice daily. GPI analysis was then performed with cultured fetal liver cells and with the residual fetal tissues, which remained after dissection of the liver, to calculate the relative contribution of *c-jun*$^{-/-}$ ES cells to the liver in relation to the average chimerism.

The contribution of *c-jun*$^{-/-}$ ES cells to the various tissues of chimeric mice at various age after birth was furthermore determined by PCR using the primers c-jun 1430 and c-jun 2287 (Table I). Hepatocytes were isolated from livers of 8-wk-old chimeric mice by collagenase liver perfusion essentially as described by Seglen (1976) except that perfusion was performed via the left ventricle (Edström et al., 1983). This technique yields a hepatocyte preparation with ~90% purity (as estimated by immunohistochemical detection of keratin), and, based on trypan blue exclusion, >85% viability. For preparation of bile ducts, sections of snap-frozen livers were stained with methylene blue, and bile ducts were microdissected under a stereo-microscope using a 25-G needle attached to an 1-ml syringe. The microdissected tissue was collected in an Eppendorf tube and DNA was isolated for PCR analysis. PCR products were separated on ethidium bromide–stained agarose gels and band intensities were estimated by video densitometry. Nonlinearity of band intensity ratios was corrected with a standard curve (Eferl et al., 1997).

## *Simultaneous Detection of S-Phase Cells and Apoptotic Cells in Fetal Liver Cell Cultures*

Livers from E12.5 mouse fetuses were mechanically dissociated and plated onto plastic chamber slides (NUNC, Kamstrup, DK) in DME containing 10% FCS. Liver cells were cultured for 2 wk in order to remove hematopoietic cells. Purity of cultured hepatoblasts was controlled by keratin immunostaining using rabbit antibodies to keratins 8 and 18, showing that more than 95% of the cells were keratin positive. Primary fibroblasts from E12.5 fetuses were cultured as described (Robertson, 1987). [$^3$H]thymidine labeling was performed with 300 kBq methyl [$^3$H]thymidine/ml medium (Amersham). Primary hepatocytes were labeled for 2 h, fibroblasts for 1 h at 37°C followed by an incubation step in medium without [$^3$H]thymidine for 30 min. Thereafter cells were rinsed twice with medium and PBS and fixed with 4% paraformaldehyde in PBS, pH 7.4, for 30 min at room temperature. Apoptotic cells were stained with the in situ cell death detection kit (Boehringer Mannheim). After dehy-

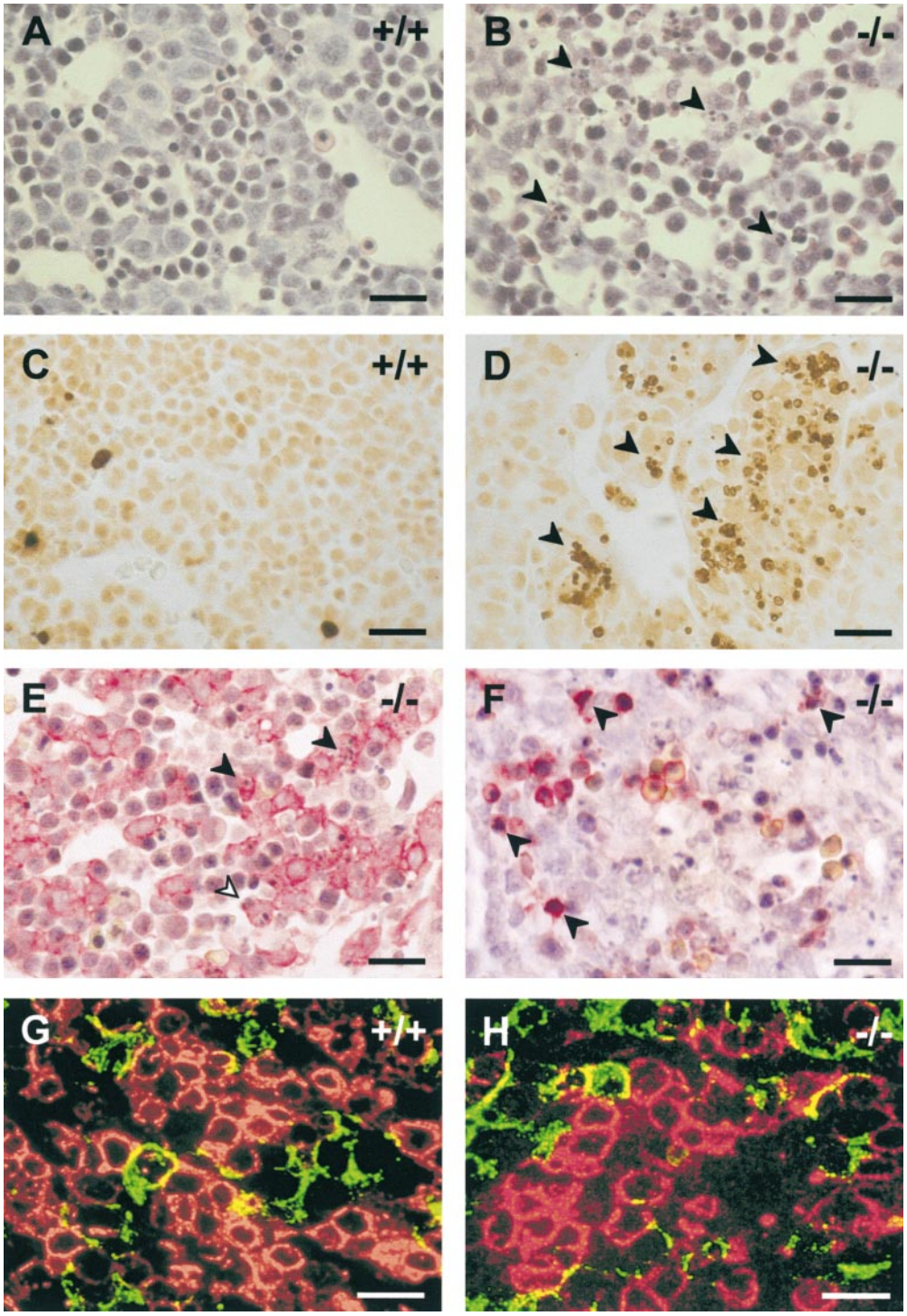


*Figure 1.* Apoptosis and distribution of hepato- and erythropoiesis in livers of *c-jun*$^{-/-}$ mouse fetuses. Liver sections of E13.0 wild-type (+/+, A and C) and homozygous *c-jun* knockout ($^{-/-}$, B and D–F) littermates. The HE-stained sections (A and B) show numerous cells with condensed nuclei, typical for apoptotic cells (arrowheads in B) in *c-jun*$^{-/-}$ livers. These nuclei contain fragmented DNA, as demonstrated by TUNEL staining (C and D, arrowheads in D). The cell types that undergo apoptosis were characterized using rabbit antibodies to keratins 8/18 (E) and the monoclonal rat antibody TER119 (F), respectively. Bound antibodies were detected by the APAAP procedure and sections were counterstained with HE. In E hepatoblasts with fragmented nuclei (filled arrowheads) and hepatoblasts with intact nuclei are visible. Some of the hepatoblasts contain apoptotic bodies (open arrowhead) engulfed by phagocytosis. In F TER119-positive erythroid cells containing fragmented nuclei are shown (arrowheads). Distribution of hepatopoiesis and erythropoiesis in livers of E12.5 wild-type (+/+, G) and *c-jun*$^{-/-}$ littermates ($^{-/-}$, H). Liver sections were double-labeled with antibodies to hepatoblasts and erythroid cells using rabbit antibodies to keratins 8 and 18 (green) and the monoclonal rat antibody TER119 (red), respectively. Bars, 20 μm.

dration with increasing concentrations of ethanol [$^3$H]thymidine-labeled cells were visualized with Kodak NTB2 photoemulsion and detected with Kodak D19 developer.

## *Results*

### *Apoptosis of Hepatoblasts and Erythroid Cells in Fetal Livers Lacking c-jun*

Previous studies revealed no readily detectable differences in development or morphology between wild-type and *c-jun*$^{-/-}$ fetuses at least up to E11.5 (Johnson et al., 1993; Hilberg et al., 1993). Between E11.5 and E14.5, in some *c-jun*$^{-/-}$ fetuses rounded hepatoblasts, which were detached from each other and scattered cells with characteristic features of apoptosis and necrosis, were detected (Hilberg et al., 1993). However, the cell types that are affected primarily in the absence of c-Jun had not been determined yet and the developmental stage at which c-Jun becomes essential for liver development was unclear. To address these questions, detailed histological analyses of fetal livers from E12.5 and E13.0 *c-jun*$^{-/-}$ fetuses were performed.

At E12.5, no morphologic abnormalities were observed in *c-jun*$^{-/-}$ livers. At E13.0, however, 8 out of 19 *c-jun*$^{-/-}$ fetuses showed increased apoptosis in the livers when compared with wild-type littermates (Fig. 1, A and B). In two of these *c-jun*$^{-/-}$ fetuses, apoptosis was very extensive, affecting up to one-third of all liver cells. Staining by in situ DNA end labeling (TUNEL) revealed fragmented DNA present in the condensed nuclei of cells undergoing apoptosis (Fig. 1, C and D). Characterization of the affected cell type by immunohistochemical staining with antibodies against keratins 8 and 18, which is expressed in hepatoblasts, and the erythroid-specific antibody TER119 confirmed, that condensed and fragmented nuclei typical of early apoptosis were present in hepatoblasts and in erythroid cells (Fig. 1, E and F). However, cells in advanced stages of apoptosis could not be classified by this method. But from the high number and distribution of apoptotic cells it is likely that apoptosis affects hepatoblasts as well as erythroid cells.

Until E12.5, hepatic erythropoiesis appeared normal since immunohistological analyses of livers using the erythroid-specific antibody TER119 (Fig. 1, G and H) and an antibody to CD71, a marker which is present in high amounts on erythroid cells, revealed no differences in the number and distribution of erythroid cells between *c-jun*$^{+/+}$ and *c-jun*$^{-/-}$ E12.5 fetuses. Moreover, macrophages, as demonstrated by staining with antibody to CD11b (Mac-1) and CD34-positive cells, were also present in comparable amounts (data not shown). This suggests that c-Jun is not required for proper establishment of hepatic hematopoiesis but rather is essential for its maintenance.

At around E11.5, the liver becomes the primary site of hematopoiesis and liver cells are necessary to provide the proper microenvironment to support survival of hematopoietic cells (Dzierzak and Medvinsky, 1995). The apoptosis observed in *c-jun*$^{-/-}$ erythroblasts could either be due to a cell-autonomous defect in this particular cell lineage or, alternatively, *c-jun*$^{-/-}$ fetal liver cells may be unable to provide the proper microenvironment for hematopoietic cells. To discriminate between these two possibilities and in order to investigate whether *c-jun*$^{-/-}$ hematopoietic cells were affected in a cell-autonomous manner, E12.5 *c-jun*$^{-/-}$ fetal liver cells were injected intravenously into wild-type lethally irradiated syngeneic adult mice. After six months, mice reconstituted with *c-jun*$^{-/-}$ cells were healthy and flow cytometric analysis of spleen, bone marrow, and thymus of two mice showed a similar distribution of myeloid and lymphoid cells as the controls (Fig. 2 A and data not shown). Analysis of peripheral blood showed no significant differences in hematocrits and red blood cell counts (data not shown). PCR analysis of genomic DNA isolated from bone marrow, spleen, and thymus of the reconstituted mice confirmed that these organs had been mostly colonized by *c-jun*$^{-/-}$ hematopoietic cells (Fig. 2 B). These results indicate that hematopoietic cells of all lineages are present and functional in *c-jun*$^{-/-}$ fetal livers, which excludes an absolute cell-autonomous defect. Therefore, the observed apoptosis in the erythroid lineage might be caused by non–cell-autonomous alterations, such as a disturbance of the microenvironment in *c-jun*$^{-/-}$ fetal livers which is essential to sustain hematopoiesis.

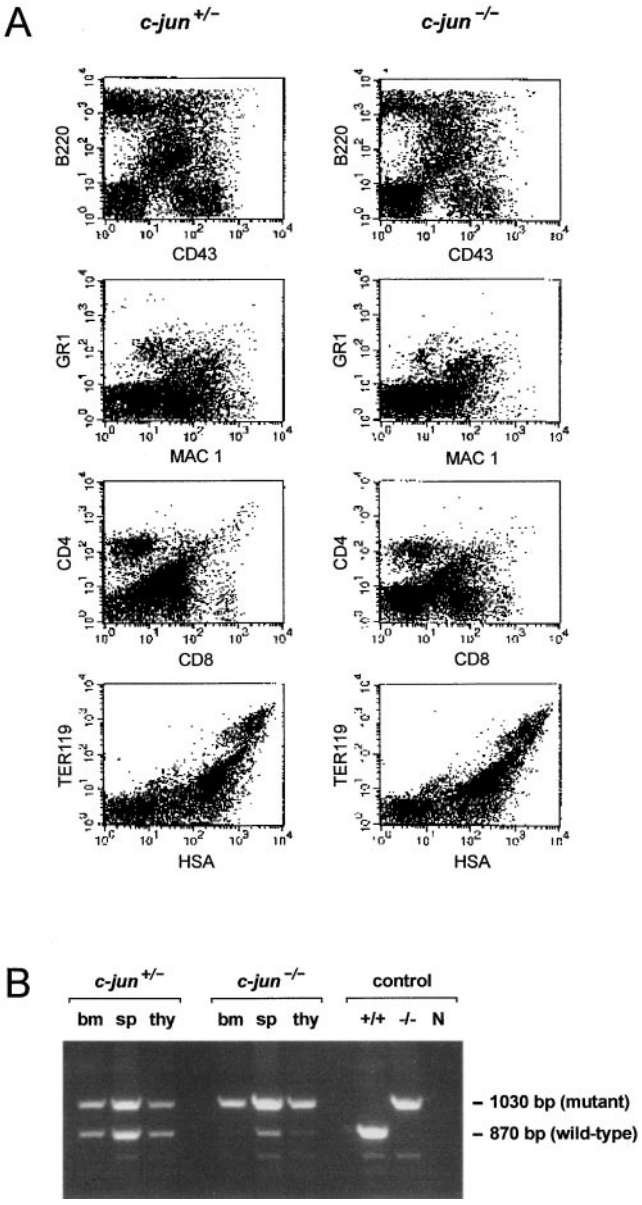


*Figure 2.* Reconstitution of hematopoiesis in lethally irradiated mice by *c-jun*$^{-/-}$ cells. (A) The hematopoietic compartment of a lethally irradiated mouse was reconstituted with *c-jun*$^{+/-}$ (left column) and *c-jun*$^{-/-}$ (right column) fetal liver hematopoietic cells and then analyzed by flow cytometry analysis of the spleen cells. The following antibodies to cell surface markers were used: B220 for B cells, CD43 for leukocytes, GR1 for granulocytes, Mac1 for macrophages, CD4 and CD8 for T cells, TER119 for erythroid cells, and heat stable antigen (HSA) for lymphoid precursor cells. (B) PCR analysis of genomic DNA isolated from bone marrow (bm), spleen (sp), and thymus (thy) of mice reconstituted with *c-jun*$^{+/-}$ and *c-jun*$^{-/-}$ hematopoietic cells. The genotype of the donor fetal liver cells is indicated above, and the size of the PCR products, derived from mutant and wild-type alleles on the right side. For control, PCR was performed with DNA from *c-jun*$^{+/+}$ (+/+) and *c-jun*$^{-/-}$ (−/−) mice, and without DNA (N).

## *Lack of c-Jun Does Not Impair Fetal Liver Gene Expression*

An altered hepatic microenvironment in *c-jun*$^{-/-}$ fetuses

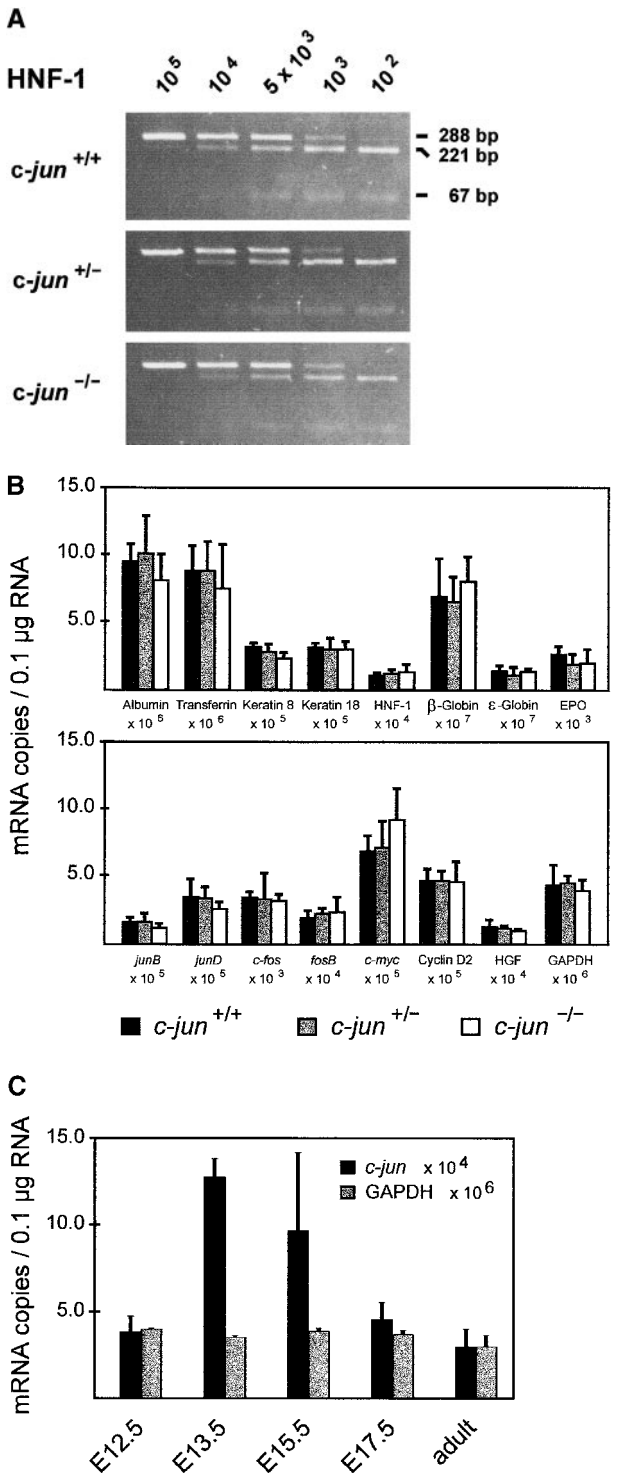


*Figure 3.* Analysis of mRNA expression in E12.5 wild-type (*c-jun*$^{+/+}$), heterozygous (*c-jun*$^{+/-}$), and homozygous *c-jun*–deleted (*c-jun*$^{-/-}$) fetal livers by quantitative RT-PCR. (A) Ethidium bromide–stained agarose gels showing quantitative RT-PCR of hepatocyte nuclear factor 1 (HNF-1) mRNA in E12.5 fetal livers. The amount of HNF-1 mRNA was estimated by a titration assay with decreasing copy numbers of RNA standard molecules (indicated at the top of the figure) and a constant amount of liver RNA (0.1 μg). Cleaved PCR products (221 bp, 67 bp) are derived from HNF-1 mRNA; noncleaved PCR products (288 bp) are derived from the RNA standard. (B) Quantitative RT-PCR of mRNAs in E12.5 fetal livers. The bars represent mean values of mRNA copy numbers per 0.1 μg RNA of at least three independent experiments. The standard deviations are indicated. HNF-1, hepatocyte nuclear factor 1; EPO, erythropoietin; HGF, hepatocyte growth factor; GAPDH, glyceraldehyde-3-phosphate dehydrogenase. (C) Expression of *c-jun* mRNA during liver development. The amount of *c-jun* mRNA was estimated by quantitative RT-PCR in wild-type mouse livers of different age (E12.5-adult). Glyceraldehyde-3-phosphate dehydrogenase (GAPDH) mRNA was estimated as control.

could be the consequence of deregulated gene expression in liver cells. Therefore, we analyzed the expression patterns of genes that are either known to be regulated by AP-1 or serve as indicators for hepatoblast differentiation and function. Since only small amounts of RNA can be obtained from E12.5 livers, we established and validated a variety of quantitative RT-PCR assays for estimation of mRNA concentrations (Eferl et al., 1997). This technique allowed analysis of several mRNAs in single fetal livers of littermates. The expression of differentiation markers for hepatoblasts, like hepatocyte nuclear factor-1 (HNF-1), and keratins 8 and 18, as well as the expression of genes involved in growth regulation, namely, the mRNAs for hepatocyte growth factor (HGF), *c-myc* and cyclin D2 was unaffected in *c-jun*$^{-/-}$ livers (Fig. 3, A and B). Moreover, the mRNA levels for secreted liver proteins as indicators for liver cell function, such as serum albumin and transferrin, did not differ between *c-jun*$^{+/+}$, *c-jun*$^{+/-}$, and *c-jun*$^{-/-}$ livers (Fig. 3 B). To see whether the ablation of c-Jun modified the expression of other Jun and Fos family members in order to compensate the loss of c-Jun functions we further analyzed the expression levels of *junB*, *junD*, *c-fos*, and *fosB*. None of these genes revealed altered expression in *c-jun*$^{-/-}$ mice (Fig. 3 B).

In addition to the analysis of possible alteration of gene expression in hepatoblasts, we investigated possible effects of the absence of c-Jun in erythroid cell. Because at around E12.0 there is the shift from embryonic ϵ-globin to adult β-globin expression, we analyzed the expression levels of β-globin and ϵ-globin mRNAs. The ratio as well as the total mRNA concentrations for both globins were similar in wild-type, *c-jun*$^{+/-}$ and *c-jun*$^{-/-}$ mice (Fig. 3 B), which is in line with the immunofluorescence data demonstrating a proper establishment of hepatic hematopoiesis. We further analyzed the expression of erythropoietin, which is the most important growth and survival factor for erythroid cells. The liver is expected to be the major site of erythropoietin synthesis during late fetal development, and decreased amounts of this factor could be responsible for apoptosis of erythroid cells as observed in *c-jun*$^{-/-}$ livers. (Koury et al., 1988). Using quantitative RT-PCR we show here that erythropoietin is expressed already in E12.5 fetal livers, although at a very low level. Furthermore, the analyses revealed no difference in the erythropoietin mRNA copy numbers between *c-jun*$^{+/+}$ and *c-jun*$^{-/-}$ livers, indicating that erythropoietin synthesis is not decreased in *c-jun*$^{-/-}$ mice.

It is surprising that all mRNAs analyzed, including mRNAs of genes that are known to be regulated by AP-1, such as keratin 18 (Oshima et al., 1990) and β-globin (Ney

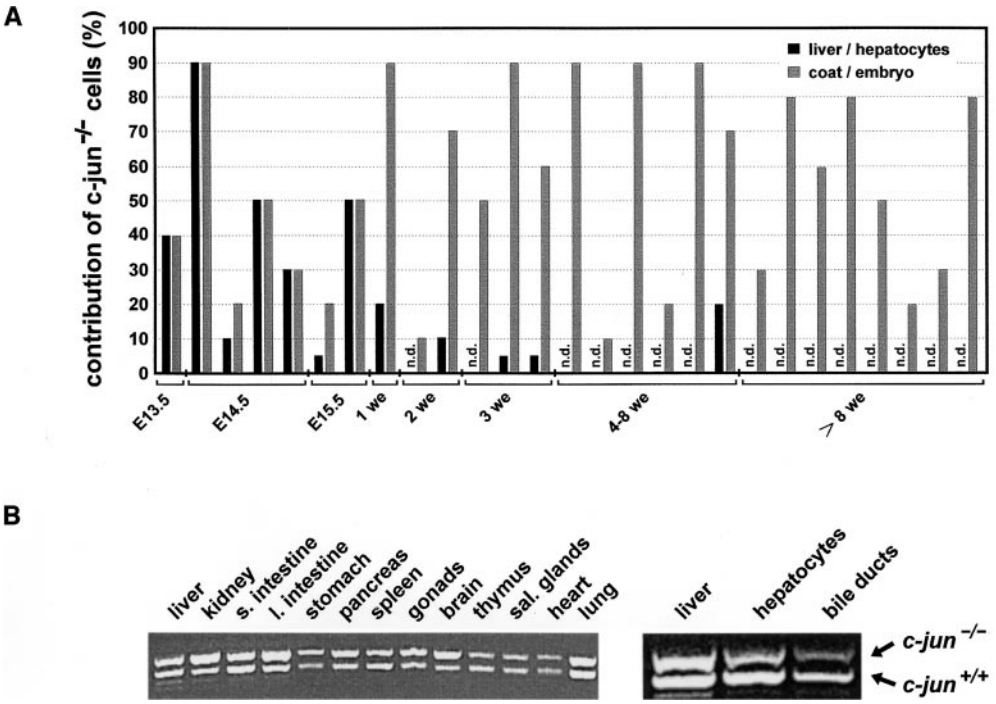


*Figure 4.* Contribution of *c-jun*$^{-/-}$ ES cells to tissues of chimeric mice. (A) Glucose phosphate isomerase (GPI) analysis of chimeric mice during fetal (E13.5–E15.5) and postnatal development (1–8 wk). The chimerism was determined by densitometric analysis of the GPI-1$^{a}$ (derived from *c-jun*$^{-/-}$ ES cells) and the GPI-1$^{b}$ isoforms (derived from the wild-type C57BL/6 blastocysts) on a cellugel. Black bars represent the amount (%) of *c-jun*$^{-/-}$ cells in fetal hepatoblasts and postnatal livers. Gray bars represent the relative contribution of *c-jun*$^{-/-}$ cells to the fetus or the skin as indicator of average chimerism. Each pair of black and gray bars are data from one chimeric animal (n.d.; no *c-jun*$^{-/-}$ cells were detectable). Presence of *c-jun*$^{-/-}$ hepatoblasts during fetal development was analyzed in short-term cultures of fetal liver cells and average chimerism was determined in the residual fetus (after removal of the liver). During postnatal development, GPI analysis was directly performed on liver tissue and coat chimerism was assessed by estimation of the coat colors (agouti versus black fur). (B) PCR analysis of *c-jun*$^{-/-}$ ES cell contribution to tissues of an 8-wk-old chimeric mouse. *c-jun*$^{+/+}$ and *c-jun*$^{-/-}$ alleles were competitively amplified by PCR from DNA of the indicated tissues (band positions on the right). Hepatocytes were isolated by collagenase perfusion. Bile ducts were microdissected under a stereomicroscope from methylene blue-stained frozen liver sections. Note that at 8 wk of postnatal development *c-jun*$^{-/-}$ cells are present in the liver and among purified hepatocytes. s. intestine, small intestine; l. intestine, large intestine; sal. glands, salivary glands.

et al., 1990), showed no significantly deregulated expression levels in E12.5 livers. One explanation is that at E12.5, when these analyses were performed, *c-jun* is expressed at a very low level ($3 \times 10^4$ copies per 0.1 μg RNA) in the liver (Fig. 3 C), and there is an up to threefold induction of *c-jun* in the liver at E13.5-E15.5 (Fig. 3 C), which coincides with the observed apoptosis of hepatoblasts and erythroid cells as well as the death of *c-jun*$^{-/-}$ fetuses. This indicates that c-Jun gains significance in the liver around E13.5 possibly by exerting functions that are not essential in earlier phases of fetal development.

### *ES Cells Lacking c-jun Contribute to the Liver of Young but Not Adult Chimeric Mice*

Previous studies of chimeric mice that were generated by injection of ES cells lacking *c-jun* into wild-type mouse blastocysts showed that the ES cells contributed to all tissues except to the liver (Hilberg et al., 1993), suggesting that in the absence of c-Jun no mature hepatocytes can be generated. However, the morphologic as well as molecular characterization of liver differentiation and function revealed no striking differences between *c-jun*$^{+/+}$ and *c-jun*$^{-/-}$ fetuses up to E12.5 (Figs. 1 and 3), which poses the question up to which developmental stage *c-jun*$^{-/-}$ hepatoblasts are able to survive and differentiate properly in chimeric mice. Analysis of *c-jun*$^{-/-}$ ES cell contribution in E14.5-E17.5 chimeric mouse livers was performed in short-term fetal liver cell cultures. A short culturing period of the fetal livers allowed us to remove most of the hematopoietic cells, which adhere much less efficiently to the culture dishes than hepatoblasts. In these cultures similar amounts of *c-jun*$^{+/+}$ and *c-jun*$^{-/-}$ hepatoblasts were detected by GPI assay (Fig. 4 A). ES cell derivatives lacking *c-jun* were also present in chimeric mouse livers at several weeks after birth (Fig. 4 A). Detailed analysis of the various tissues from an 8-wk-old chimeric mouse by PCR showed substantial contribution of *c-jun*$^{-/-}$ cells to the liver cell mass (Fig. 4 B). These *c-jun*$^{-/-}$ cells were present among the hepatocyte cell population, which was isolated and enriched by collagenase liver perfusion, ensuring that the *c-jun*$^{-/-}$ cells did not reflect nonparenchymal cells, like sinusoidal endothelial or Kupffer cells. Moreover, bile duct epithelial cells were analyzed after enrichment by microdissection. Since we found substantial contribution of *c-jun*$^{-/-}$ cells to bile duct epithelia, the absence of c-Jun has no obvious adverse effect on the differentiation of hepatoblasts into the hepatocytic or the bile duct epithelial lineage. There was, however, a tendency of continuous loss of *c-jun*$^{-/-}$ hepatocytes in older chimeric mice. *c-jun*$^{-/-}$ hepatocytes were detectable up to 8 wk after birth but not in 3-mo-old or older mice. This points to an imbalance in the regulation of hepatocyte cell turnover in adult mice in that *c-jun*$^{-/-}$ hepatocytes have either a proliferation or a survival disadvantage over wild-type hepatocytes.

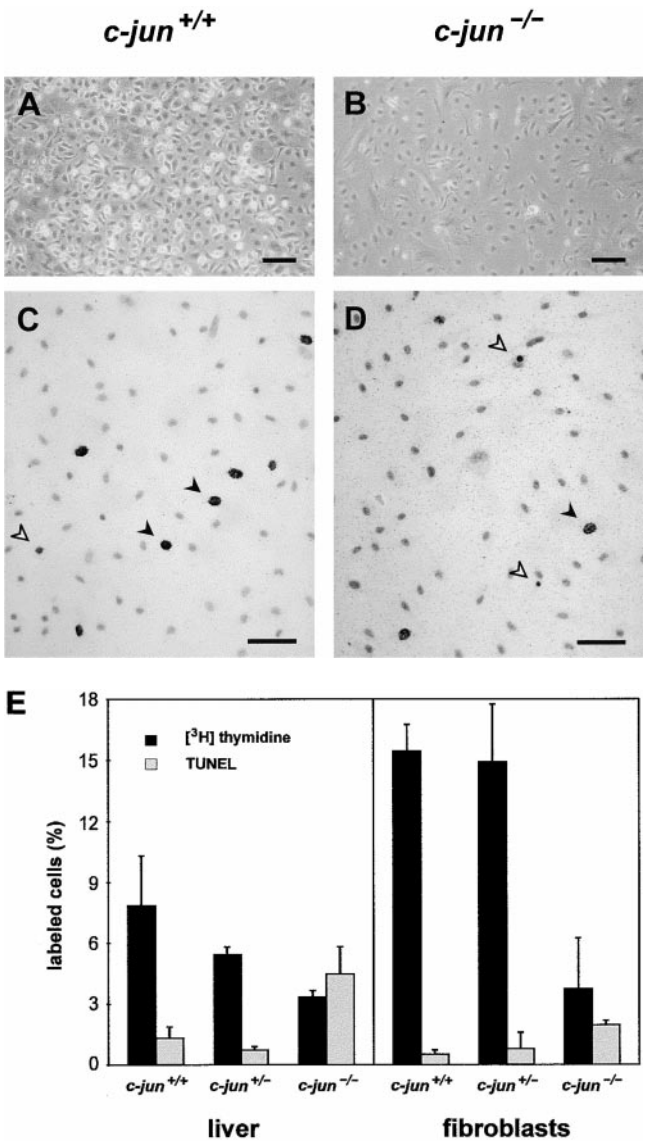


*Figure 5.* Growth of fetal liver cells lacking *c-jun*. (A and B) Primary liver cultures from E12.5 *c-jun*$^{+/+}$ and *c-jun*$^{-/-}$ littermates. Note the reduced cell number and density in cultures from *c-jun*$^{-/-}$ livers (B). Bars: 100 μm. (C and D) Simultaneous detection of apoptosis and DNA replication in E12.5 fetal liver cultures. Primary hepatoblasts were stained for apoptotic cells by TUNEL (open arrowheads) and for cells replicating its DNA by [$^3$H]thymidine incorporation (filled arrowheads). The number of apoptotic cells is increased in *c-jun*$^{-/-}$ cultures (D) whereas the number of [$^3$H]thymidine-labeled cells is reduced. (E) Percentage of [$^3$H]thymidine-labeled cells (dark bars) and apoptotic cells (light bars) in E12.5 primary liver cells and corresponding fibroblast cultures. Note the three- to fourfold increased apoptosis and reduced number of [$^3$H]thymidine-labeled cells in *c-jun*$^{-/-}$ cultures of primary hepatocytes and fibroblasts. The bars represent mean values of three to six independent experiments using separate fetuses for preparation of liver and fibroblast cultures. The standard deviations are indicated. Bars, 50 μm.

### *Increased Apoptosis and Reduced Cell Growth of c-jun*$^{-/-}$ *Fetal Hepatocytes In Vitro*

A possible impact of the loss of c-Jun on hepatocyte cell turnover, namely, on proliferation capacity and apoptotic rate, was analyzed in primary cell cultures of E12.5 *c-jun*$^{+/+}$ and *c-jun*$^{-/-}$ livers. The purity control of these cultures by immunohistochemical detection of keratin expression showed presence of >95% keratin positive cells in *c-jun*$^{+/+}$ as well as in *c-jun*$^{-/-}$ cultures (data not shown). The growth rates and the achieved cell densities were markedly reduced in *c-jun*$^{-/-}$ cultures (Fig. 5, A and B). Simultaneous staining of S-phase and apoptotic cells by combined [$^3$H]thymidine incorporation and TUNEL reaction revealed approximately four times increased apoptosis of *c-jun*$^{-/-}$ hepatoblasts (Fig. 5, C–E). Concomitant with the increase in the number of apoptotic cells the number of S-phase cells was decreased to ~50%. Analysis of fibroblast cultures established in parallel from E12.5 fetuses yielded essentially similar results. These findings show that c-Jun is an important proliferation regulator of hepatoblasts and fibroblasts, and that in addition to the reduced mitotic capacity the increase in apoptotic rates is a major factor contributing to the reduced growth potential of both cell types. The data obtained in vitro together with the observation that several *c-jun*$^{-/-}$ E13.0 fetuses showed increased apoptoses of erythroblasts and hepatoblasts in their livers, point to an essential role of c-Jun in the regulation of apoptosis in a diversity of cell types in vitro and in vivo.

### *Lack of c-jun Affects the Development of the Outflow Tract in the Fetal Heart*

Deregulation of apoptosis in the absence of c-Jun was not evident at E12.5, whereas at E13.0 an increase of apoptosis was noted in 42% (8/19) of the *c-jun*$^{-/-}$ livers. It appears that apoptosis of liver cells occurs only shortly before death of the fetuses and, therefore, can be missed if fetuses are not examined at the appropriate time point. However, some of the fetuses died without substantial apoptotic rates in their livers. Thus, apoptosis of hepatoblasts and erythroid cells in the livers of *c-jun*$^{-/-}$ fetuses cannot explain fetal lethality in all cases. This prompted us to look for additional defects in *c-jun*$^{-/-}$ fetuses. Histological analysis of E12.5 fetuses by horizontal serial sections revealed defective development of the heart in all (19/19) of the investigated *c-jun*$^{-/-}$ fetuses (Fig. 6, A and B). The animals showed a malformation of the outflow tract with a single outflow vessel that arose entirely from the right ventricle resembling the congenital human heart malformation of a persistent truncus arteriosus (incomplete separation of the aorta and the pulmonary artery). In addition to this anomaly of the outflow tract we found in some animals an abnormal remodeling of the aortic arch arteries resulting in a right-sided aortic arch. Moreover, the wall of the right ventricle was constantly thinner and the endocardial cushion material of the bulbus arteriosus appeared more prominent in c-Jun knockout mice as compared to wild-type mice. These alterations could, in principle, also reflect a delay in heart development rather than a true malformation. However, a mere developmental delay is very unlikely since we could analyze two *c-jun*$^{-/-}$ fetuses which survived until E14.5 and had heart defects. These fetuses showed a malformation of the outflow tract with only one common outflow vessel that arose from the right ventricle, had an abnormal positioning of the aortic arch, and re-

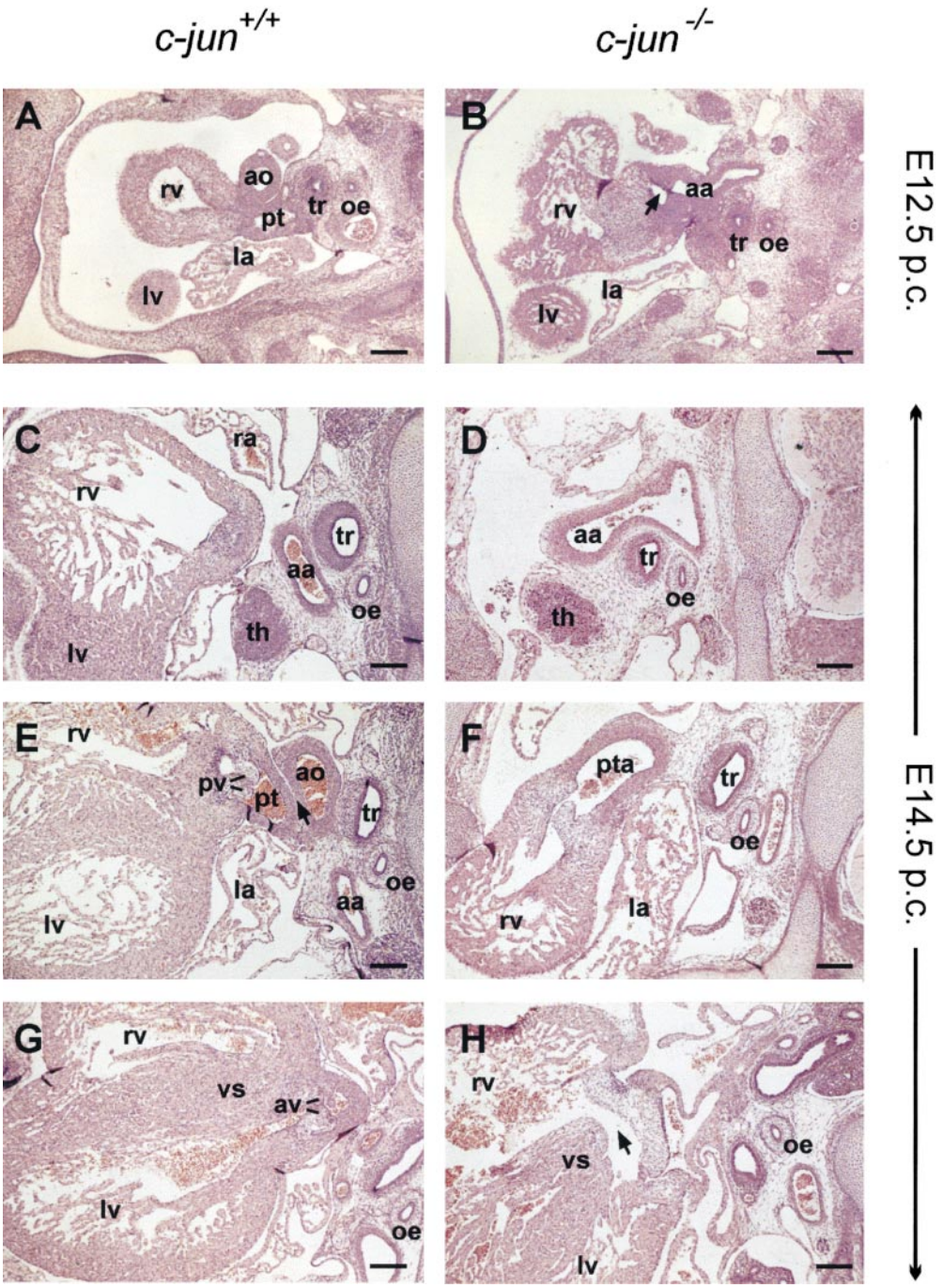


*Figure 6.* Impaired heart development of *c-jun*$^{-/-}$ fetuses. Corresponding horizontal sections of E12.5 wild-type (A) and *c-jun*$^{-/-}$ mouse fetuses (B) were stained with HE. At this stage of development, wild-type fetuses show separation of the aorta (ao) and the pulmonary trunk (pt). In *c-jun*$^{-/-}$ fetuses (B) there is a single outflow vessel (arrow) that arises from the right ventricle. Corresponding horizontal sections through the hearts of E14.5 wild-type (C, E, and G) and *c-jun*$^{-/-}$ mouse fetuses (D, F, and H). The sections are arranged from cranial to caudal and show three major anomalies: (a) persistence of the right branch of the 4th aortic arch artery (aa in D), (b) persistent truncus arteriosus (pta in F) whereas the wild-type littermate show complete separation of the aorta and pulmonary trunk (arrow in E), and (c) incomplete septation of the ventricles (arrow in H). ao, aorta; pt, pulmonary trunk; rv, right ventricle; lv, left ventricle; ra, right atrium; la, left atrium; aa, aortic arch; tr, trachea; oe, oesophagus; th, thymus; pv, pulmonary valve; pta, persisting truncus arteriosus; av, aortic valve; vs, ventricular septum. Bars, 200 μm.

vealed a wide connection between the left and right ventricle. In contrast, *c-jun*$^{+/+}$ E14.5 littermates had a regularly developed aorta ascendens and pulmonary trunk as well as showed complete septation of the left and right ventricles (Fig. 6, C–H).

Since there is a general concept that malformations of the heart outflow tract are due to neural crest cell defects, and similar malformations were described in mice defective in genes necessary for neural crest cell development or migration (Kirby and Waldo, 1995; Rossant, 1996), we analyzed possible alterations of the contribution of neural crest cells to the peritracheal and cardiac mesenchyme. Neural crest cells were detected by immunohistochemical staining of Cx 43 (Fig. 7, A–F). The analysis showed that neural crest cells expressing the marker Cx 43 were present in *c-jun*$^{-/-}$ mice and had properly migrated from the spinal cord to the mesenchyme surrounding the trachea. There was, however, a difference between wild-type and *c-jun*$^{-/-}$ mice in that fewer Cx 43 positive cells were detected in the outflow tract of the right ventricle of mutant mice. Although the direct comparison of Cx 43–expressing cells in wild-type and *c-jun*$^{-/-}$ mice is hampered because of the differences in the anatomy of the outflow tracts, the immunofluorescence data are in good

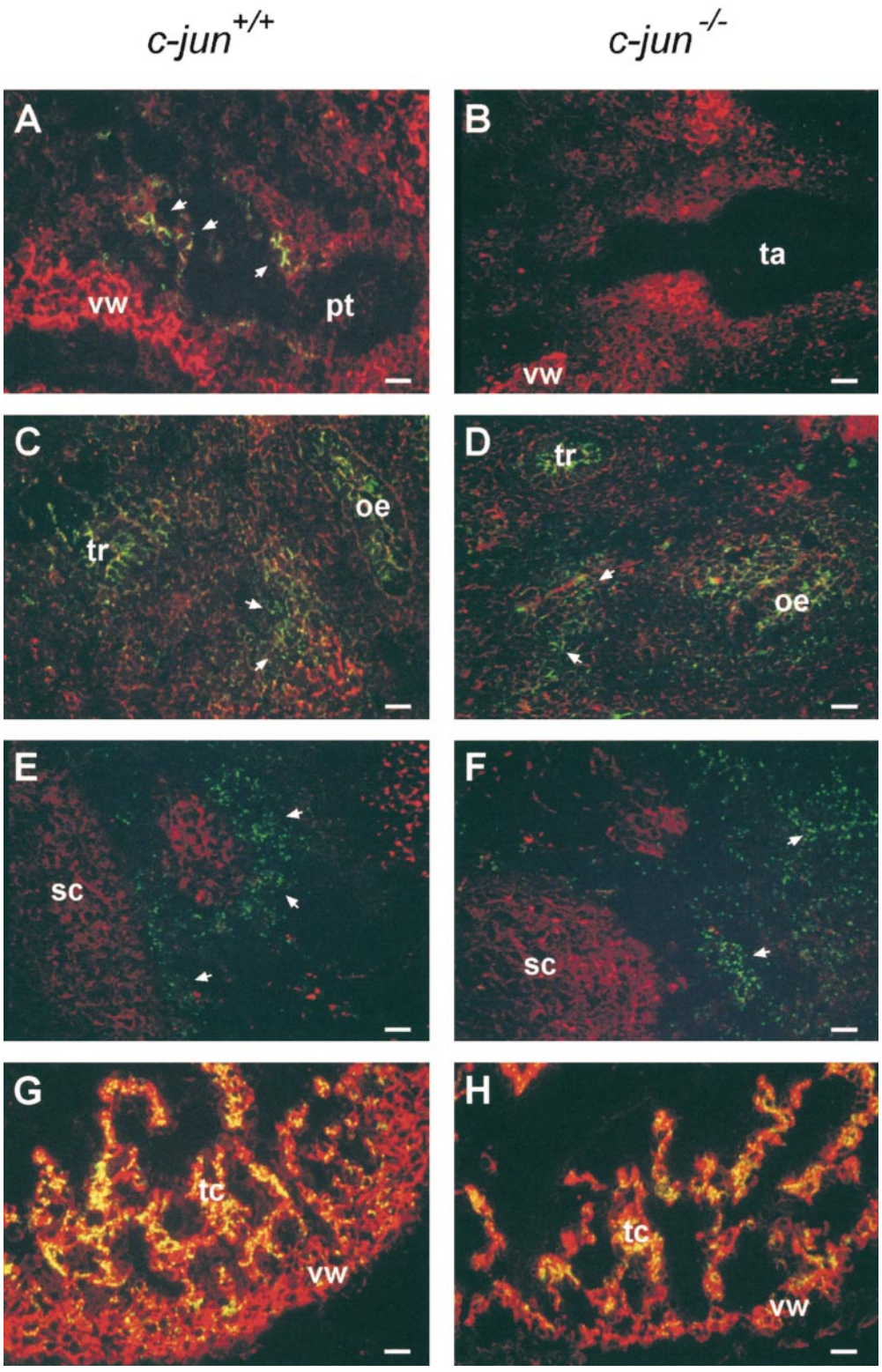


*Figure 7.* Impaired migration of neural crest cells to the outflow tracts of *c-jun*$^{-/-}$ fetuses. Corresponding horizontal sections of E12.5 wild-type (A, C, E, and G) and *c-jun*$^{-/-}$ mouse fetuses (B, D, F, and H) were analyzed for the presence of neural crest cells by double-label immunofluorescence microscopy using a monoclonal mouse antibody against the neural crest cell protein Cx 43 (green) and polyclonal antibodies against desmin (red). The micrographs show corresponding sections of *c-jun*$^{+/+}$ (A, C, E, and G) and *c-jun*$^{-/-}$ (B, D, F, and H) littermates (two *c-jun*$^{+/+}$, one *c-jun*$^{+/-}$, and four *c-jun*$^{-/-}$ fetuses were analyzed). Cx 43 positive cells were visible in the outflow tract of wild-type (arrows in A) but not in *c-jun*$^{-/-}$ fetuses (B). In contrast to the outflow tract, no differences in Cx 43 immunoreactivity were found between wild-type and *c-jun*$^{-/-}$ fetuses in the peritracheal mesenchyme (arrows in C and D) and the mesenchyme in vicinity of the spinal cord (arrows in E and F). For control, Cx 43 immunoreactivity is shown in the trabeculae carneae of the ventricles (G and H). Note the thinner wall of the ventricles in *c-jun*$^{-/-}$ hearts (H). pt, pulmonary trunk; ta, truncus arteriosus; vw, ventricle wall; tr, trachea; oe, oesophagus; sc, spinal cord; tc, trabeculae carneae. Bars, 50 μm.

accordance with the observed spectrum of heart malformations that are typical for a neural crest cell defect.

## *Discussion*

*c-jun* is one of the earliest genes that is transcribed after stimulation of cells with growth factors and during tissue regeneration. A central role of c-Jun in the regulation of cell proliferation has been underlined by previous findings with cultured *c-jun*$^{-/-}$ fibroblasts that had markedly reduced proliferation capacities (Hilberg et al., 1993; Johnson et al., 1993; Schreiber et al., 1999). In vivo, however, lack of c-Jun did not lead to growth defects in fetuses but caused mid-gestational lethality that was suggested to

be due to a liver defect (Hilberg et al., 1993). Until E12.5 of fetal development, no obvious liver defects were observed in the absence of c-Jun and the expression levels of 15 different mRNAs were similar in wild-type and *c-jun* mutant mice. At E13.0, however, numerous apoptoses were seen in the liver of *c-jun*$^{-/-}$ fetuses and lethality occurred. These alterations coincided with the time of *c-jun* mRNA induction in the liver indicating that c-Jun exerts a specific function in liver development at this stage, and that in the absence of c-Jun, erythroblasts and hepatoblasts undergo apoptosis. A cell-autonomous defect as the primary and only cause of erythroblast apoptosis was ruled out by the ability of hematopoietic precursor cells isolated from E12.5 *c-jun*$^{-/-}$ livers to fully reconstitute all hematopoietic lineages in lethally irradiated mice. Thus apoptoses of erythroblasts in homozygous *c-jun* deleted livers cannot be exclusively the consequence of the absence of c-Jun in erythroblasts themselves, but most likely involves additional exogenous factors, such as an altered microenvironment in *c-jun*$^{-/-}$ fetal livers, that do not allow maintenance of hematopoiesis. This microenvironment that has to be provided by the cells of the fetal liver is yet poorly characterized. It might resemble the microenvironment generated by stromal cells of the bone marrow in adult animals. Stromal cells secrete a variety of growth factors that stimulate proliferation and differentiation of hematopoietic cells as well as protect them from apoptosis. One of these growth factors is erythropoietin, which is an essential, and probably the most important survival factor for erythroid cells. Mice carrying loss of function mutations of erythropoietin or the erythropoietin receptor suffered from anemia and died at around E13.5, revealing numerous apoptoses of erythroid cells in their livers, thus resembling in part the alterations seen in *c-jun* knockout mice (Wu et al., 1995). Because the liver is expected to be the major site of erythropoietin synthesis during fetal development, functional deficiencies in *c-jun*$^{-/-}$ livers could result in reduced erythropoietin levels. However, RT-PCR results revealed that in E12.5 *c-jun*$^{-/-}$ fetuses, the erythropoietin mRNA concentrations were not altered, so apoptoses of erythroid cells cannot be explained by decreased erythropoietin synthesis. Moreover, a general impairment of erythropoietin signaling in the absence of c-Jun was excluded by the reconstitution experiments in which cells without functional c-Jun properly differentiated into erythrocytes. So far, we could not further specify the mechanism that caused apoptosis of erythroblasts in *c-jun*$^{-/-}$ mice, and besides deficiencies in erythropoietin, alterations in the expression or function of a variety of other growth factors as well as changes in cell–cell and cell–matrix interactions must be considered.

The effect of c-Jun inactivation was not restricted to erythroid cells but also affected other cell types, such as hepatoblasts and fibroblasts. Primary liver cell as well as fibroblast cultures established from E12.5 *c-jun*$^{-/-}$ fetuses and their corresponding wild-type littermates showed markedly increased apoptotic rates in the absence of c-Jun. This was surprising, since in contrast to our findings, previous studies reported that overexpression of c-Jun forced fibroblasts into apoptosis, and functional inhibition of c-Jun prevented cell death in some cell types (Estus et al., 1994; Ham et al., 1995; Bossy-Wetzel et al., 1997). These controversial observations indicate that the role of c-Jun in apoptosis depends on the cellular context and mode of treatment. It is interesting that in *c-jun*$^{-/-}$ mice no obvious alteration of apoptosis was noted during fetal development until E11.5, whereas primary cell cultures derived from E12.5 *c-jun*$^{-/-}$ mice had markedly increased apoptotic rates. One possible explanation for this difference between the in vivo and in vitro situation is that apoptosis is preferentially triggered under enforced stimulation of proliferation as it is the case under cell culture conditions. It is possible that the absence of c-Jun modulates the intracellular signals induced by growth factors so that cells respond with apoptosis instead of mitosis. In addition to the alterations in apoptosis, we noted reduced mitotic rates in primary cultures of *c-jun*$^{-/-}$ fibroblasts and hepatoblasts. One mechanism by which lack of c-Jun could result in impaired proliferation was recently shown by Schreiber et al., 1999. The proliferation defect in *c-jun*$^{-/-}$ fibroblast cell lines was found to be p53-dependent, indicating that the alterations of proliferation, and probably also the increased propensity of cells to undergo apoptosis may involve p53-dependent pathways.

The altered regulation of cell proliferation and apoptosis in the absence of c-Jun could be an explanation for the occurrence of massive apoptosis of erythroblasts and hepatoblasts in *c-jun*$^{-/-}$ E13.0 fetuses. Moreover, the proliferation defect as well as the increase in apoptosis could lead to the loss of *c-jun*$^{-/-}$ cells in livers of adult chimeric mice because of a lower capacity of *c-jun*$^{-/-}$ hepatocytes to contribute to the cell turnover. However, it is unlikely that the deregulation of proliferation and apoptosis is the only cause of fetal lethality since massive apoptosis was seen in only 2 livers out of 19 *c-jun*$^{-/-}$ fetuses, and we have analyzed some *c-jun*$^{-/-}$ fetuses that had died in utero without showing severe morphological liver alterations.

It is known from other gene knockout mice, that in addition to the liver, defects in other organ systems, especially the cardiovascular system, have to be considered as causes of mid-gestational lethality (Rossant, 1996). Detailed investigation of hearts of *c-jun*$^{-/-}$ fetuses revealed a novel function for c-Jun in fetal heart development. Lack of c-Jun led to several anomalies of the heart outflow tracts. All of the *c-jun*$^{-/-}$ fetuses had compared with wild-type littermates anomalies of the aorta ascendens and pulmonary artery in that in mutant mice there was a single outflow vessel arising from the right ventricle resembling a truncus arteriosus persistens. In addition to the outflow tract alteration, some mice showed a right-sided aortic arch. These anomalies are typical for a neural crest cell defect (Kirby and Waldo, 1995). It has been shown that the ectomesenchymal cells of cardiac neural crest, which extends from the midotic placode to the caudal limit of somite 3, migrate into the outflow tract of the heart where they contribute to the aorticopulmonary septum. Moreover, cardiac neural crest cells differentiate into smooth muscle cells of the aortic arch and contribute to the stroma of other derivatives of the pharyngeal arches such as thymus, parathyroid, and thyroid gland (Kirby and Waldo, 1990). Experimental ablation of neural crest cells in chick embryos led to various defects of which a persistent truncus arteriosus was a common denominator. These lesions were always combined with a ventricular septal defect (Nishibatake et al., 1987).

Furthermore, a right-sided aortic arch or anomalies of the other great arteries were seen after partial neural crest cell ablation.

The cardiovascular defects observed by us in c-Jun knockout mice were almost identical to those found after neural crest cell ablation in chicken. Similar to the observations in chicken, a variety of gene mutant mice with impaired neural crest cell development showed anomalies of the outflow tract. For instance, the mouse mutant Splotch, which harbors a mutation in the homeobox gene *pax3*, exhibits conotruncal and aortic arch defects (Conway et al., 1997; for review on mouse mutants with heart defects see Olson and Srivastava, 1996). In contrast to the situation in chicken and in the above-mentioned mouse mutant, where cardiac neural crest cell were either absent or had a general defect, we have observed no difference in neural crest cell distribution in *c-jun* knockout mice except for a reduced number of Cx 43–expressing cells in the outflow tract of the right ventricle. This observation suggests that the consequences of c-Jun inactivation primarily affects neural crest cell function in the heart and does not result in a general neural crest cell defect. As known from neural crest cell ablation experiments in animals as well as from human diseases with a truncus arteriosus persistens (e.g., DiGeorge syndrome), the malformations are not restricted to the heart but also affect other neural crest cell derivatives, such as the thymus or parathyroid. In *c-jun* mutant fetuses, however, morphologic analysis provided no evidence for a thymus defect, and thus for a general alteration of the cardiac neural crest (Fig. 6, C and D). Nevertheless, the cardiac malformations observed are highly reminiscent for a disturbance of neural crest function, which may be restricted to the heart and great vessels. Moreover, as shown by neural crest cell transplantation experiments, the mere presence of neural crest cells does not exclude functional deficiencies (Kirby and Waldo, 1990).

The cardiac malformation of a truncus arteriosus persistens may be a major factor contributing to the lethal phenotype. In principle, occurrence of a truncus arteriosus persistens is compatible with survival because of compensation of the hemodynamic imbalance. This compensation may not occur in *c-jun* mutant fetuses and fetal lethality might be due to pleiotropic defects reflecting the diversity of functions of c-Jun in development, such as a role in neural crest cell function, in the maintenance of hepatic hematopoiesis and in the regulation of apoptosis.

The technical assistance of Ms. C. Stumptner is gratefully acknowledged.

This work has been supported by a grant from the Austrian Science Foundation (S7401-MOB) to K. Zatloukal and E.F. Wagner (S07406-MOB). R. Zenz is supported by a scholarship of the Austrian Academy of Sciences.

Received for publication 23 October 1998 and in revised form 14 April 1999.

*References*

Angel, P., I. Baumann, B. Stein, H. Delius, H.J. Rahmsdorf, and P. Herrlich. 1987. 12-O-tetradecanoyl-phorbol-13-acetate induction of the human collagenase gene is mediated by an inducible enhancer element located in the 5′-flanking region. *Mol. Cell. Biol.* 7:2256–2266.

Behrens, A., M. Sibilia, and E.F. Wagner. 1999. Amino-terminal phosphorylation of c-Jun regulates stress-induced apoptosis and cellular proliferation. *Nat. Genet.* 21:326–329.

Bengal, E., L. Ransone, R. Scharfmann, V.J. Dwarki, S.J. Tapscott, H. Weintraub, and I.M. Verma. 1992. Functional antagonism between c-Jun and MyoD proteins: a direct physical association. *Cell.* 68:507–519.

Bossy-Wetzel, E., L. Bakiri, and M. Yaniv. 1997. Induction of apoptosis by the transcription factor c-Jun. *EMBO (Eur. Mol. Biol. Organ.) J.* 16:1695–1709.

Conway, S.J., D.J. Henderson, M.L. Kirby, R.H. Anderson, and A.J. Copp. 1997. Development of a lethal congenital heart defect in the splotch (pax3) mutant mouse. *Cardiovasc. Res.* 36:163–173.

Desmet, V.J. 1998. Ludwig symposium on biliary disorders part I: pathogenesis of ductal plate abnormalities. *Mayo. Clin. Proc.* 73:80–89.

Dzierzak, E., and A. Medvinsky. 1995. Mouse embryonic hematopoiesis. *Trends Genet.* 11:359–366.

Edström, S., L. Ekman, M. Ternell, and K. Lundholm. 1983. Isolation of mouse liver cells: perfusion technique and metabolic evaluation. *Eur. Surg. Res.* 15: 97–102.

Eferl, R., M. Lehner, L. Kenner, I. Kapfer, B. Guertl, and K. Zatloukal. 1997. Evaluation of different RNA standards for quantitative reverse transcription PCR: possible pitfalls and strategies for avoidance. *Elsevier Trends Journals Technical Tips Online.* http://tto.biomednet.com, T01214.

Estus, S., J. Zaks, R.S. Freeman, M. Gruda, R. Bravo, and E.M. Johnson, Jr. 1994. Altered gene expression in neurons during programmed cell death: identification of *c-jun* as necessary for neuronal apoptosis. *J. Cell Biol.* 127: 1717–1727.

Gaub, M.P., M. Bellard, I. Scheuer, P. Chambon, and P. Sassone-Corsi. 1990. Activation of the ovalbumin gene by estrogen receptor involves the fos-jun complex. *Cell.* 63:1267–1276.

Grigoriadis, A.E., Z.-Q. Wang, M.G. Cecchini, W. Hofstetter, R. Felix, H.A. Fleisch, and E.F. Wagner. 1994. C-Fos: a key regulator of osteoclast-macrophage lineage determination and bone remodeling. *Science.* 266:443–448.

Ham, J., C. Babij, J. Whitfield, C.M. Pfarr, D. Lallemand, M. Yaniv, and L.L. Rubin. 1995. A *c-jun* dominant negative mutant protects sympathetic neurons against programmed cell death. *Neuron.* 14:927–939.

Hilberg, F., A. Agguzi, N. Howells, and E.F. Wagner. 1993. c-Jun is essential for normal mouse development and hepatogenesis. *Nature.* 365:179–181.

Johnson, R.S., B.M. Spiegelman, and V. Papaioannou. 1992. Pleiotropic effects of a null mutation in the c-fos proto-oncogene. *Cell.* 71:577–586.

Johnson, R.S., B. van Lingen, V.E. Papaioannou, and B.M. Spiegelman. 1993. A null mutation at the *c-jun* locus causes embryonic lethality and retarded cell growth in culture. *Genes Dev.* 7:1309–1317.

Jonat, C., H.J. Rahmsdorf, K.-K. Park, A.C.B. Cato, S. Gebel, H. Ponta, and P. Herrlich. 1990. Antitumor promotion and antiinflamation: down-modulation of AP-1 (Fos/Jun) activity by glucocorticoid hormone. *Cell.* 62:1189–1204.

Kerr, L.D., J.T. Holt, and L.M. Matrisian. 1988. Growth factors regulate transin gene expression by c-fos-dependent and c-fos-independent pathways. *Science.* 242:1424–1427.

Kirby, M.L., and K.L. Waldo. 1990. Role of neural crest in congenital heart disease. *Circulation.* 82:332–340.

Kirby, M.L., and K.L. Waldo. 1995. Neural crest and cardiovascular patterning. *Circ. Res.* 77: 211–215.

Koury, M.J., M.C. Bondurant, S.E. Graber, and S.T. Sawyer. 1988. Erythropoietin messenger RNA levels in developing mice and transfer of $^{125}$I-erythropoietin by the placenta. *J. Clin. Invest.* 82:154–159.

Krieg, P., E. Amtmann, and G. Sauer. 1983. The simultaneous extraction of high-molecular-weight DNA and of RNA from solid tumors. *Anal. Biochem.* 134:288–294.

Kuo, C.J., P.B. Conley, C.L. Hsieh, U. Francke, and G.R. Crabtree. 1990. Molecular cloning, functional expression, and chromosomal localization of mouse hepatocyte nuclear factor 1. *Proc. Natl. Acad. Sci. USA.* 87:9838–9842.

Lazo, P.S., K. Dorfman, T. Noguchi, M.G. Mattei, and R. Bravo. 1992. Structure and mapping of the fosB gene. FosB downregulates the activity of the fosB promoter. *Nucleic Acids Res.* 20:343–350.

Lee, W., P. Mitchell, and R. Tjian. 1987. Purified transcription factor AP-1 interacts with TPA-inducible enhancer elements. *Cell.* 49:741–752.

Liu, Y., G.K. Michalopoulos, and R. Zarnegar. 1993. Molecular cloning and characterization of cDNA encoding mouse hepatocyte growth factor. *Biochim. Biophys. Acta.* 1216:299–303.

Matsushime, H., M.F. Roussel, R.A. Ashmun, and C.J. Sherr. 1991. Colony-stimulating factor 1 regulates novel cyclins during the G1 phase of the cell cycle. *Cell.* 65:701–713.

Minghetti, P.P., S.W. Law, and A. Dugaiczyk. 1985. The rate of molecular evolution of alpha-fetoprotein approaches that of pseudogenes. *Mol. Biol. Evol.* 2:347–358.

Morita, T., M.L. Tondella, Y. Takemoto, K. Hashido, Y. Ichinose, M. Nozaki, and A. Matsushiro. 1988. Isolation of EndoA cDNA from mouse 8-cell stage embryo. *Biochem. Res. Commun.* 154:890–894.

Ney, P.A., B.P. Sorrentino, K.T. McDonagh, and A.W. Nienhuis. 1990. Tandem AP-1 binding sites within the human beta-globin dominant control region function as an inducible enhancer in erythroid cells. *Genes Dev.* 4:993–1006.

Nishibatake, M., M.L. Kirby, and L.H.S. van Mierop. 1987. Pathogenesis of persistent truncus arteriosus and dextroposed aorta in the chick embryo after neural crest ablation. *Circulation.* 75:255–264.

Olson, E.N., and D. Srivastava. 1996. Molecular pathways controlling heart development. *Science.* 272:671–676.

Oshima, R.G., L. Abrams, and D. Kulesh. 1990. Activation of an intron enhancer within the keratin 18 gene by expression of c-fos and *c-jun* in undifferentiated F9 embryonal carcinoma cells. *Genes Dev.* 4:835–848.

Robertson, E.J. 1987. Teratocarcinomas and Embryonic Stem Cells: A Practical Approach. E.J. Robertson, editor. IRL, Oxford. 113–151.

Roffler-Tarlov, S., J.J.G. Brown, E. Tarlov, J. Stolarov, D.L. Chapman, M. Alexiou, and V.E. Papaioannou. 1996. Programmed cell death in the absence of cFos and c-Jun. *Development.* 122:1–9.

Rossant, J. 1996. Mouse mutants and cardiac development: new molecular insights into cardiogenesis. *Circ. Res.* 78:349–353.

Ruppert, S., M. Boshart, F.X. Bosch, W. Schmid, R.E.K. Fournier, and G. Schütz. 1990. Two genetically defined trans-acting loci coordinately regulate overlapping sets of liver-specific genes. *Cell.* 61:895–904.

Ryder, K., and D. Nathans. 1988. Induction of proto-oncogene *c-jun* by serum growth factors. *Proc. Natl. Acad. Sci. USA.* 85:8464–8467.

Ryder, K., L.F. Lau, and D. Nathans. 1988. A gene activated by growth factors is related to the oncogene v-jun. *Proc. Natl. Acad. Sci. USA.* 85:1487–1491.

Ryder, K., A. Lanahan, E. Perez-Albuerne, and D. Nathans. 1989. junD: A third member of the jun gene family. *Proc. Natl. Acad. Sci. USA.* 86:1500–1503.

Sabath, D., H.E. Broome, and M.B. Prystowsky. 1990. Glyceraldehyde-3-phosphate dehydrogenase mRNA is a major interleukin 2-induced transcript in a cloned T-helper lymphocyte. *Gene.* 91:185–191.

Schorpp-Kistner, M., Z.Q. Wang, P. Angel, and E.F. Wagner. 1999. JunB is essential for mammalian placentation. *EMBO (Eur. Mol. Biol. Organ.) J.* 18: 934–948.

Schreiber, M., A. Kolbus, F. Piu, A. Szabowski, U. Möhle-Steinlein, J. Tian, M. Karin, P. Angel, and E.F. Wagner. 1999. Control of cell cycle progression by c-Jun is p53-dependent. *Genes Dev.* 13:607–619.

Schüle, R., K. Umesono, D.J. Mangelsdorf, J. Bolado, J.W. Pike, and R.M. Evans. 1990. Jun/Fos and receptors for vitamin A and D recognize a common response element in the human osteocalcin gene. *Cell.* 61:497–504.

Seglen, P.O. 1976. Preparation of isolated rat liver cells. *Methods Cell Biol.* 13: 29–83.

Shehee, W.R., D.D. Loeb, N.B. Adey, F.H. Burton, N.C. Casavant, P. Cole, C.J. Davis, R.A. McGraw, S.A. Schichman, D.M. Severynse, et al. 1989. Nucleotide sequence of the BALB/c mouse beta-globin complex. *J. Mol. Biol.* 205:41–62.

Shoemaker, C.B., and L.D. Mitsock. 1986. Murine erythropoietin gene: cloning, expression, and human gene homology. *Mol. Cell Biol.* 6:849–858.

Sibilia, M., and E.F. Wagner. 1995. Strain-dependent epithelial defects in mice lacking the EGF receptor. *Science.* 269:234–238.

Sibilia, M., J.P. Steinbach, L. Stingl, A. Agguzi, and E.F. Wagner. 1998. A strain-independent postnatal degeneration in mice lacking the EGF receptor. *EMBO (Eur. Mol. Biol. Organ.) J.* 17:719–731.

Singer, P.A., K. Trevor, and R.G. Oshima. 1986. Molecular cloning and characterisation of the EndoB cytokeratin expressed in implanted mouse embryos. *J. Biol. Chem.* 261:538–547.

Stanton, L.W., P.D. Fahrlander, P.M. Tesser, and K.B. Marcu. 1984. Nucleotide sequence comparison of normal and translocated murine c-myc genes. *Nature.* 310:423–425.

van Beveren, C., F. van Straaten, T. Curran, R. Müller, and I.M. Verma. 1983. Analysis of FBJ-MuSV provirus and c-fos (mouse) gene reveals that viral and cellular fos gene products have different carboxy termini. *Cell.* 32:1241–1255.

Wang, Z.Q., C. Ovitt, A.E. Grigoriadis, U. Mohle-Steinlein, U. Ruther, and E.F. Wagner. 1992. Bone and haematopoietic defects in mice lacking c-fos. *Nature.* 360:741–745.

Wu, H., X. Liu, R. Jaenisch, and H.F. Lodish. 1995. Generation of committed erythroid BFU-E and CFU-E progenitors does not require erythropoietin or the erythropoietin receptor. *Cell.* 83:59–67.

Zatloukal, K., H. Denk, G. Spurej, E. Lackinger, K.-H. Preisegger, and W.W. Franke. 1990. High molecular weight component of mallory bodies detected by a monoclonal antibody. *Lab. Invest.* 62:427–434.